Studying Pyrene-Labeled Macromolecules with the Model-Free Analysis

Michael A. Fowler,[†] Jean Duhamel,*,[†] Greg J. Bahun,[‡] Alex Adronov,[‡] Gerardo Zaragoza-Galán,[§] and Ernesto Rivera[§]

[†]Institute of Polymer Research, Waterloo Institute of Nanotechnology, Department of Chemistry, University of Waterloo, Waterloo, Ontario N2L 3G1, Canada

[‡]Department of Chemistry and the Brockhouse Institute for Materials Research, McMaster University, Hamilton, Canada

[§]Instituto de Investigaciones en Materiales, Universidad Nacional Autónoma de México, Ciudad Universitaria, 04510 D.F. México

Ⓢ *Supporting Information*

ABSTRACT: The model-free (MF) analysis was applied to the fluorescence decays of 32 pyrene-labeled macromolecules to probe their internal dynamics. Depending on whether a pyrene derivative was attached to the chain ends of a linear chain, randomly along a polymer backbone, or at the chain terminals of dendrimers, the MF analysis was applied to probe the dynamics of polymer ring closure, backbone flexibility, or chain terminal mobility, respectively. For those polymeric constructs whose decays could be fitted according to Birks' scheme or the fluorescence blob model (FBM), good agreement was obtained between the rate constant for excimer formation retrieved from the MF analysis $\langle k^{MF} \rangle$ and those obtained according to the Birks' scheme or FBM analyses. The MF analysis was also applied to conduct the first successful direct comparison of the chain terminal dynamics of two types of pyrene end-labeled dendrons. Finally, the MF analysis was employed to build a calibration curve against which the internal dynamics of any pyrene-labeled macromolecule can now be benchmarked. This study further confirms the versatility and robustness of the MF analysis to study any type of pyrene-labeled macromolecule.
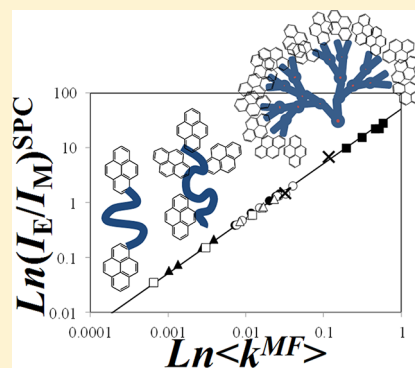
INTRODUCTION

Excimer formation between pyrenyl groups covalently attached onto macromolecules yields information about the extent of translational diffusion undergone by the units of the macromolecule bearing the pyrenyl pendants, which in turn reflects the internal dynamics of the macromolecule that undergoes a conformational rearrangement to enable the diffusive encounter of the pyrenyl pendants.[1−5] Careful design of the synthetic protocol applied to covalently attach a pyrenyl derivative onto a macromolecule enables one to probe the effect that a given molecular parameter such as chain length or chain flexibility for a linear polymer[1−4] or internal crowding for a dendrimer[5] has on the macromolecule considered. For instance, attachment of pyrene to the chain ends of a series of linear monodisperse polymers[1,6−11] or alkyl chains[12−14] of different chain lengths provides information about the effect of chain length on the rate constant of ring closure. Linear chains randomly labeled with pyrene can be used to assess how the chemical structure of a monomer affects the internal dynamics of the resulting polymer.[3,15−20] Labeling the chain ends of dendrimers of different generations enables one to probe the chain end dynamics as crowding of the dendrimer interior increases with increasing generation number.[21−26] These examples represent the most developed uses of pyrene excimer formation to characterize a specific aspect of the internal dynamics of

different macromolecules and they have been summarized in a number of reviews.[1−5]

In each study, the process of excimer formation is characterized by a rate constant which is obtained by fitting the pyrene monomer and excimer fluorescence decays acquired with a pyrene-labeled macromolecule with an appropriate model. DMD model,[27] Birks' scheme,[1,28] Fluorescence blob model (FBM),[3,15] and model-free (MF) analysis[5,26] are typically applied to determine the rate constant of pyrene excimer formation for pyrene end-labeled alkyl chains, pyrene end-labeled linear chains, linear chains randomly labeled with pyrene, and pyrene end-labeled dendrimers, respectively. Out of these four analyses, the MF analysis has been touted as being capable of handling any type of macromolecular architecture labeled with pyrene.[4] This report investigates the validity of this claim by applying the MF analysis to two series of pyrene end-labeled linear chains, three series of polystyrenes randomly labeled with pyrene, and two series of pyrene end-labeled dendrons, and comparing the rate constant of pyrene excimer formation $\langle k^{MF} \rangle$ obtained by the MF analysis to k_{cy} obtained with the Birks scheme for the end-labeled linear chains and the

Table 1. Pyrene Contents Expressed As the Molar Fraction x in Mol % of Pyrene-Labeled Monomer and λ_{Py} in μmol·g^{-1}, Number-Average Molecular Weights, and PDIs

Sample structure	Sample name	x mol% Py	λ_{Py} μmol.g^{-1}	M_n kg.mol^{-1}	PDI
	CoEt-PS-MPy	1.5	141	35	1.81
		1.8	169	45	1.87
		3.2	284	32	1.99
		4.8	412	16	1.85
		5.1	436	34	1.80
		6.4	533	46	1.65
	CoAm-PS-MPy	1.1	105	43	1.88
		2.5	230	39	2.04
		3.7	331	55	1.90
		5.0	437	28	1.88
		5.2	459	34	1.96
		6.4	550	39	1.91
	CoEs-PS-BuPy	2.1	190	46	1.65
		3.1	280	43	1.67
		4.5	390	49	1.62
		5.4	467	53	1.69
		6.0	510	46	1.68
	PS-BuPy$_2$	1.6 [a]	157 [a]	12.7 [a]	1.20 [a]
		2.6	250	8.0	1.09
		4.6	444	4.5	1.12
		6.9	667	3.0	1.10
	PEO-MPy$_2$	0.5	113	16.5	1.05
		0.9	184	10.0	1.05
		1.8	350	5.0	1.08
		4.4	800	2.0	1.10
	PP-G1-BuPy$_2$	n.a.	2,967	0.67	1.0
	PP-G2-BuPy$_4$	n.a.	2,766	1.45	1.0
	PP-G3-BuPy$_8$	n.a.	2,676	2.99	1.0
	PP-G4-BuPy$_{16}$	n.a.	2,632	6.08	1.0
	PP-G4-BuPy$_{16}$ (purified by GPC[15])	n.a.	2,632	6.08	1.0
	PA-G1-BuPy$_2$	n.a.	3,221	0.62	1.0
	PA-G2-BuPy$_4$	n.a.	2,905	1.38	1.0

[a] These samples yielded too little excimer to determine the $(I_E/I_M)^{SS}$ ratio with sufficient accuracy.

product $k_{blob} \times N_{blob}$ obtained with the FBM for the randomly labeled linear chains. Considering that the MF analysis does not make any assumption on the modeling details used to describe excimer formation, the good agreement reported herein between $\langle k^{MF} \rangle$, k_{cy}, and $k_{blob} \times N_{blob}$ is remarkable. This agreement consolidates the claim that the MF analysis can be applied to any type of pyrene-labeled macromolecule. In particular, it validates the use of the MF analysis to conduct the first comparison of the chain end dynamics of two different types of pyrene end-labeled dendrons. Possibly, more importantly, the MF analysis was used to generate a universal scale for the ratio of the fluorescence intensity of the excimer I_E over that of the monomer I_M obtained from the MF analysis of the fluorescence decays acquired by the single photon counting (SPC) method, namely, the $(I_E/I_M)^{SPC}$ ratio, against which the $(I_E/I_M)^{SPC}$ ratio of any other pyrene-labeled macromolecule can now be compared.

■ EXPERIMENTAL SECTION

The chemical structure of all pyrene-labeled macromolecules considered is shown in Table 1. These macromolecules include three series of polydisperse polystyrene constructs randomly labeled with pyrene (CoEt-PS-MPy and CoAm-PS-MPy labeled with a 1-pyrenemethyl derivative[29] and CoEt-PS-BuPy labeled with a 1-pyrenebutyl derivative[30]), a series of monodisperse polystyrenes end-labeled with 1-pyrenebutyl-amine (PS-BuPy$_2$),[18] a series of monodisperse poly(ethylene oxide) end-labeled with 1-pyrenemethanol (PEO-MPy$_2$),[11] a series of 1−4 generation dendrons made of a bis-(hydroxymethyl)propionic acid backbone end-labeled with 1-pyrenebutyric acid (PP-G1-BuPy$_2$, PP-G2-BuPy$_4$, PP-G3-BuPy$_8$, PP-G4-BuPy$_{16}$)[30] and two polyaryl Fréchet-type dendrons labeled with 1-pyrenebutanol (PA-G1-BuPy$_2$ and PA-G2-BuPy$_4$).[31] Together, these pyrene-labeled macromolecules offer a variety of molecular architectures between linear chains (CoEt-PS-MPy, CoAm-PS-MPy, CoEs-PS-BuPy, PS-BuPy$_2$, PEO-MPy$_2$) and branched dendrons (PP-G1-BuPy$_2$, PP-G2-BuPy$_4$, PP-G3-BuPy$_8$, PP-G4-BuPy$_{16}$, PA-G1-BuPy$_2$,

and PA-G2-BuPy$_4$), modes of labeling between labeling at the ends (PS-BuPy$_2$, PEO-MPy$_2$, PP-G1-BuPy$_2$, PP-G2-BuPy$_4$, PP-G3-Py$_8$, PP-G4-Py$_{16}$, PA-G1-BuPy$_2$, and PA-G2-BuPy$_4$) and randomly along the chain (CoEt-PS-MPy, CoAm-PS-MPy, CoEs-PS-BuPy) and types of pyrene labels between derivatives of 1-pyrenemethyl (CoEt-PS-MPy, CoAm-PS-MPy, PEO-MPy$_2$) and 1-pyrenebutyl (CoEs-PS-BuPy, PS-BuPy$_2$, PP-G1-BuPy$_2$, PP-G2-BuPy$_4$, PP-G3-BuPy$_8$, PP-G4-BuPy$_{16}$, PA-G1-BuPy$_2$, and PA-G2-BuPy$_4$). The acquisition of the steady-state fluorescence spectra and time-resolved fluorescence decays of these macromolecules have been described in earlier publications for CoEt-PS-MPy,[18] CoAm-PS-MPy,[18] CoEs-PS-BuPy,[32] PS-BuPy$_2$,[18] PEO-MPy$_2$,[11] and the pyrene-labeled PP-[26] and PA-[31] dendrimers. A brief summary of the procedures used for the photophysical studies is provided hereafter. Absorption spectra of the polymer solutions were recorded on a CARY 100 Bio UV−vis spectrophotometer or HP 8452A diode-array spectrophotometer. All solutions used for fluorescence measurements had an absorption smaller than 0.1 at 344 nm in tetrahydrofuran equivalent to a pyrene concentration of 2.5×10^{-6} mol·L^{-1}, low enough to ensure that the process of excimer formation occurs intramolecularly.

Steady-state fluorescence measurements were performed on a Photon Technology International (PTI) LS-100 steady-state fluorometer with an Ushio UXL-75Xe Xenon lamp and a PTI 814 photomultiplier detection system. To determine the ratio of the fluorescence intensity of the pyrene excimer over that of the pyrene monomer from the steady-state (SS) fluorescence spectra, namely, the $(I_E/I_M)^{SS}$ ratio, I_M and I_E were determined by taking the integral under the fluorescence spectra over the wavelength range 372−378 and 500−530 nm, respectively. Fluorescence decays were acquired using an IBH Ltd. time-resolved fluorometer equipped with an IBH 340 nm NanoLED. The samples were excited at 344 nm and the monomer and excimer fluorescence decays were acquired at 375 and 510 nm, respectively. Residual light scattering was blocked off from reaching the detector with cutoff filters at 370 and 480 nm, respectively. All decays were fitted using the MF analysis which has been described in a number of articles.[26,33−35] The decays acquired with the end-labeled linear chains (PS-BuPy$_2$ and PEO-MPy$_2$) were fitted according to the Birks scheme[1,11,18] whereas those acquired with the randomly labeled linear polystyrene (CoEt-PS-MPy, CoAm-PS-MPy, CoEs-PS-BuPy) were fitted with the FBM.[3,15,18,30] The equations used for the analysis of the fluorescence decays are provided in Supporting Information (SI). Optimization of the pre-exponential factors and decay times was accomplished with the Marquardt−Levenberg algorithm.[36] The quality of the fits was determined from the χ^2 parameter ($\chi^2 < 1.30$) and the random distribution of the residuals and the autocorrelation of the residuals. The parameters retrieved from the analysis of the fluorescence decays with the different models are listed in Tables S1−10 in SI.

■ RESULTS

The fluorescence decays of the pyrene monomer and excimer of all the pyrene-labeled macromolecules presented in this study have been acquired in earlier publications.[18,26,30,31] All decays were fitted according to the MF analysis. In the case of the end-labeled samples and the randomly labeled polystyrenes, their decays were also fitted according to, respectively, Birks' scheme and the FBM for comparison purposes. The equations used to fit the fluorescence decays have been derived

earlier[18,26,30,31] and are provided in SI. The three types of analysis fitted the fluorescence decays of the pyrene monomer and excimer globally and optimized the actual photophysical parameters used to derive the pre-exponential factors and decay times of the equations employed by each model.

The analysis of fluorescence decays acquired with pyrene-labeled macromolecules assumes that excimer formation occurs via either diffusion between an excited pyrene Py$^*_{diff}$ and a ground-state pyrene or direct excitation of a pyrene dimer E0 or D. The difference between the E0 and D dimers is whether they are constituted of two properly or improperly stacked pyrene monomers, respectively. After absorption of a photon, E0* emits as an excimer with a natural lifetime τ_{E0}, whereas D* emits with a different lifetime τ_D. Besides Py$^*_{diff}$, E0*, and D*, a fourth pyrene species often encountered when dealing with pyrene-labeled macromolecules is the species Py$^*_{free}$, which represents those pyrene monomers that do not form excimer and emit with the natural lifetime of pyrene τ_M, either because they are located in a pyrene-poor subdomain of the macromolecule[3,15,16,18−20] or they are not covalently bound to the macromolecule.[5,26,32] Whereas excimer formation is described by a single rate constant in Birks' scheme[1,6−11,28] or a distribution of rate constants in the FBM resulting from the Poisson distribution of the pyrene labels among the blobs,[3,15−20] no assumption is being made in the MF analysis regarding the actual mathematical form of the equation that describes the diffusive encounters between the pyrene labels.[4,5,26,31−33] The decay of the excimer-forming monomers is represented by a sum of exponentials ($\Sigma a_i \exp(-t/\tau_i)$) whose pre-exponential factors (a_i) and decay times (τ_i, where $\tau_i < \tau_M$) are used to predict the equations describing the excimer decay. MF analysis of the pyrene monomer and excimer decays is conducted globally and yields the molar fractions of the four pyrene species present in solution, namely, f_{diff}, f_{free}, f_{E0}, and f_D for the Py$^*_{diff}$, Py$^*_{free}$, E0*, and D* species, respectively, the excimer lifetimes τ_{E0} and τ_D, and the pre-exponential factors (a_i) and decay times (τ_i). In turn, the set of a_i and τ_i parameters is used to calculate the average rate constant of pyrene excimer formation, $\langle k^{MF} \rangle$, whose expression is given in eq 1.

$$\langle k^{MF} \rangle = \frac{1}{\langle \tau \rangle} - \frac{1}{\tau_M} \tag{1}$$

In eq 1, $\langle \tau \rangle$ is the number average lifetime of the pyrene monomer ($\Sigma a_i \tau_i / \Sigma a_i$), which excludes the contribution of Py$^*_{free}$.

Comparison of MF and Birks' Scheme Analysis. Birks' scheme was applied solely to the PEO-MPy$_2$ and PS-BuPy$_2$ samples. The main difference between an analysis based on Birks' scheme or the MF is the use of an excimer dissociation rate constant (k_{-cy}) in the former analysis.[1,28] In the latter analysis, k_{-cy} is neglected.[4,5] The analysis of the fluorescence decays acquired with pyrene end-labeled linear chains is difficult because these samples are notorious for forming very little excimer, as the chain holds the pyrene labels away from each other.[18] The weak excimer formation results in the pyrene monomer decaying in a quasi-monoexponential fashion, which complicates the recovery of the various parameters involved in the kinetic scheme. To help the MF and Birks' scheme analysis, the excimer lifetime (τ_{E0}) in the analysis of the fluorescence decays was fixed to the value recovered with the shortest PS-BuPy$_2$ (τ_{E0} = 48 ns) and PEO-MPy$_2$ (τ_{E0} = 55 ns) samples, which formed the most excimer. The results of these analyses are listed in Tables S1−3 for the MF analysis and Tables S5−7 for the Birks' scheme analysis. As typically observed for pyrene

14691

dx.doi.org/10.1021/jp307161c | *J. Phys. Chem. B* 2012, 116, 14689−14699

end-labeled polymers,[1,7−11] the k_{-cy} values recovered from the Birks' scheme analysis were small and equal to 3.7 ($\pm$0.6) $\times 10^6$ s^{-1} and 2.9 ($\pm$0.7) $\times 10^6$ s^{-1} for the PS-BuPy$_2$ and PEO-MPy$_2$ series, respectively. The small k_{-cy} values support the assumption made in the MF and FBM analysis that k_{-cy} can be neglected.

The rate constants of excimer formation k_{cy} and $\langle k^{MF} \rangle$ were determined and plotted in Figure 1 as a function of polymer
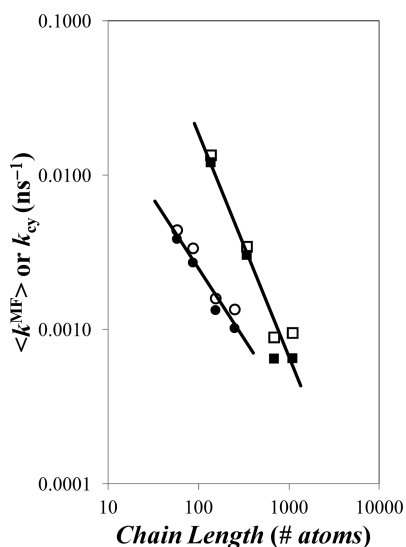
Figure 1. Plot of $\langle k^{MF} \rangle$ (filled symbols) and k_{cy} (open symbols) vs chain length for PS-BuPy$_2$ (circles) and PEO-MPy$_2$ (squares) in tetrahydrofuran. [Py] = 2.5 $\times 10^{-6}$ mol·L^{-1}.

chain length in terms of the number of atoms constituting the chains using 2 and 3 atoms for a styrene and ethylene oxide monomer, respectively. In all cases, k_{cy} was between 10 and 40% larger than $\langle k^{MF} \rangle$. As has been observed in numerous examples with k_{cy}, both data series showed a strong decrease in the rate constant of excimer formation with increasing polymer chain length.

The flexible PEO backbone made of ether bonds enables easier excimer formation than polystyrene with its bulky phenyl side group. This is clearly reflected by both k_{cy} and $\langle k^{MF} \rangle$ that, for a given chain length, take much larger values for the PEO-MPy$_2$ series than for the PS-BuPy$_2$ series. The scaling exponent (α) for k_{cy} ($\sim N^{-\alpha}$) was found to equal 0.87 ($\pm$0.13) and 1.38 ($\pm$0.23) for PS-BuPy$_2$ and PEO-MPy$_2$, respectively. Within experimental error, the same α exponents were obtained for $\langle k^{MF} \rangle$, taking values of 0.95 ($\pm$0.09) and 1.52 ($\pm$0.24) for PS-BuPy$_2$ and PEO-MPy$_2$, respectively. These exponents fall within the 0.9−1.9 range typically obtained for a Birks' scheme analysis of fluorescence decays acquired with pyrene end-labeled linear chains.[1,9,11,37]

While an excellent agreement was obtained between $\langle k^{MF} \rangle$ from the MF analysis and k_{cy} from the Birks' scheme analysis in Figure 1, it is worthwhile to point out that the α-values obtained for k_{cy} of 0.87 $\pm$ 0.13 for PS-BuPy$_2$ and 1.38 $\pm$ 0.23 for PEO-MPy$_2$ in THF are somewhat different from those of 1.62 and 0.91 $\pm$ 0.12 reported by Winnik et al.[7] and Ghiggino et al.[9] for PS in toluene and PEO in THF, respectively. In the case of PEO, the k_{cy} values obtained by Ghiggino et al. agree very well with ours, as can be seen in Figure S1. We suspect that the difference in the α-value of the exponent is a consequence of the small number of data points used in both

studies, three in the study by Ghiggino and four in our study. Combining these seven data points in Figure S1 results in an α-value of 1.18 $\pm$ 0.12, the intermediate between the two α-values of 0.91 and 1.38. In the case of polystyrene, the solvents are different. However, toluene and THF are both good solvents toward polystyrene and both have similar viscosity. Consequently, pyrene excimer formation should proceed in a similar manner in both solvents. This is indeed observed in Figure S2, where the k_{cy} values obtained by Winnik et al. compare relatively well with our values, except for the longer chains. It must be pointed that we did not include in our report a longer PS-BuPy$_2$ sample with an M_n of 15 K for which the monomer decay could hardly be distinguished from that of the model compound. For these longer chains, we find that the polymer is so long that some excited pyrenes can no longer probe the entire polymer coil. This is evidenced by the large f_{Mfree} value of 0.49 in Table S5 found for the PS-BuPy$_2$ sample with an M_n value of 13 K. A recent study has found that, under such conditions, an excited pyrene probes a subvolume of the polymer coil that is referred to as a blob and k_{cy} plateaus as it represents excimer formation inside V_{blob} and, thus, no longer depends on chain length.

In the Winnik et al. study,[7] the fluorescence decays of the pyrene monomer were fitted with two exponentials without accounting for those pyrenes that did not form excimer, namely, the Py$^*_{free}$ species. It is possible that the presence of the Py$^*_{free}$ species resulted in longer decay times that, in turn, led to smaller k_{cy} values in the study by Winnik et al. and an apparently steeper drop in k_{cy} as a function of M_n. However, these discrepancies could also be due to the small number of samples used in our study.

In any case, the purpose of the present study was not to determine the scaling law between k_{cy} and M_n, in which case a much larger number of samples would have been needed, but rather to demonstrate that the MF and Birks' scheme analysis provided similar information about the kinetics of excimer formation for end-labeled linear chains. The good agreement found in Figure 1 indicates that this is indeed the case. Considering that the MF analysis makes no assumption about the process of excimer formation, the similarity between the trends shown in Figure 1 for $\langle k^{MF} \rangle$ and k_{cy} and the ability of $\langle k^{MF} \rangle$ to report on the known flexibility of the PEO chain versus that of polystyrene is quite remarkable.

Comparison of MF and FBM Analysis. The results obtained from the MF and FBM analyses of the fluorescence decays acquired with the randomly labeled polystyrenes are listed in Tables S1−3 and S8−10, respectively. Within the FBM framework,[3,15−20] an excited pyrene probes a finite volume within the polymer coil while it remains excited. This volume is referred to as a blob or V_{blob}. V_{blob} represents a unit volume that is used to divide the polymer coil into a cluster of blobs among which the randomly attached pyrene labels distribute themselves randomly according to a Poisson distribution. Excimer formation occurs sequentially with slow diffusive encounter inside the blobs of the monomers bearing the pyrene labels, characterized by a rate constant k_{blob}, followed by a rapid rearrangement of these pyrene labels to form an excimer with a rate constant k_2. FBM analysis of the fluorescence decays yields k_{blob} and $\langle n \rangle$, the average pyrene content inside one blob. The parameter $\langle n \rangle$ is used to determine N_{blob}, the number of monomers constituting the polymer stretch encompassed inside a blob. The expression of N_{blob} is given in eq 2.

$$N_{blob} = \frac{1 - f_{Mfree}}{\lambda_{Py}} \times \frac{\langle n \rangle}{x \times M_{Py} + (1-x) \times M} \quad (2)$$

In eq 2, f_{Mfree} represents the fraction of pyrenes that do not form excimer in the pyrene monomer decay, λ_{Py} is the pyrene content listed in Table 1 and expressed in moles of pyrene per gram of polymer, and M_{Py} and M are the molar masses of the pyrene-labeled monomer and the styrene monomer, respectively. In several instances, the product $k_{blob} \times N_{blob}$ has been shown to provide a good representation of the polymer chain dynamics and remains constant with pyrene content.[20,30,38] This trend is observed in Figure 2 where the products $k_{blob} \times$
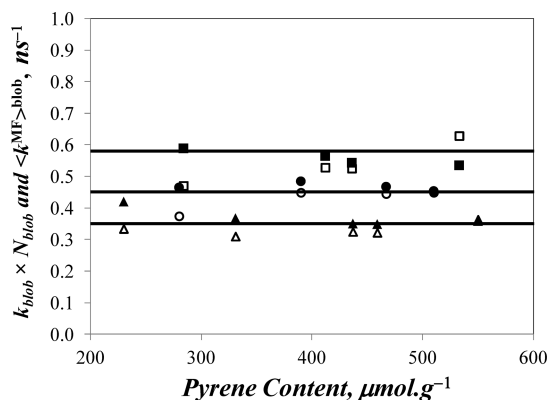

Figure 2. Plot of $k_{blob} \times N_{blob}$ (filled) and $\langle k^{MF} \rangle^{blob}$ (empty) vs pyrene content for CoEt-MPy (squares), CoEs-PS-BuPy (circles), and CoAm-PS-MPy (triangles) in tetrahydrofuran. [Py] = 2.5×10^{-6} mol·L^{-1}.

N_{blob} take values of 0.60 (± 0.05), 0.47 (± 0.01), and 0.37 (± 0.02) $\times 10^9$ s^{-1} for the CoEt-MPy, CoEs-PS-BuPy, and CoAm-PS-MPy, respectively. This trend is consistent with those published earlier[30] where the decays acquired for CoEt-MPy and CoAm-PS-MPy were fitted with a simpler version of the FBM.

According to the FBM, k_{blob} is a pseudounimolecular rate constant equal to the product of the bimolecular rate constant k_{diff} describing the diffusive encounters between two pyrene labels and the local pyrene concentration equivalent to one pyrene inside a blob, namely, $1/V_{blob}$. By comparison, $\langle k^{MF} \rangle$ obtained with the MF analysis equals the product of k_{diff} and the local pyrene concentration inside the polymer coil, which can be estimated as $\langle n \rangle / V_{blob}$. These considerations lead to eq 3 that relates the product $k_{blob} \times N_{blob}$ to the rate constant $\langle k^{MF} \rangle$.

$$
\begin{aligned}
k_{blob} \times N_{blob} &= \frac{\langle k^{MF} \rangle}{\langle n \rangle} \times N_{blob} \\
&= \frac{1 - f_{Mfree}}{\lambda_{Py}} \times \frac{\langle k^{MF} \rangle}{x \times M_{Py} + (1-x) \times M} \\
&= \langle k^{MF} \rangle^{blob} \quad (3)
\end{aligned}
$$

$\langle k^{MF} \rangle^{blob}$ was plotted in Figure 2 as a function of pyrene content for the three polystyrene series in THF. Here again the agreement between $k_{blob} \times N_{blob}$ and $\langle k^{MF} \rangle^{blob}$ is rather good, considering that no assumption is being made to obtain $\langle k^{MF} \rangle$. The value of $\langle k^{MF} \rangle^{blob}$ equals 0.56 (± 0.02), 0.43 (± 0.04), and 0.33 (± 0.02) $\times 10^9$ s^{-1} for CoEt-MPy, CoEs-PS-BuPy, and CoAm-PS-MPy, respectively. Within experimental error, $\langle k^{MF} \rangle^{blob}$ and $k_{blob} \times N_{blob}$ were found to be equivalent.

As for the product $k_{blob} \times N_{blob}$, the differences in $\langle k^{MF} \rangle^{blob}$ reflect the mode of attachment of the pyrene derivative.[30] In the case of CoEt-PS-MPy, pyrene is bound to polystyrene via a flexible ether bridge linked to the phenyl ring. Pyrene, being further away from the backbone, probes a larger V_{blob}, which results in larger $\langle k^{MF} \rangle^{blob}$ and $k_{blob} \times N_{blob}$ values in Figure 2. The amide linker connecting pyrene to the polystyrene backbone of CoAm-PS-MPy is short and rigid. Consequently, small N_{blob} values were retrieved and $\langle k^{MF} \rangle^{blob}$ and $k_{blob} \times N_{blob}$ took the smallest values. CoEs-PS-BuPy with its butyl linker holds the pyrene labels at an intermediate distance between CoAm-PS-Mpy and CoEt-PS-MPy, and intermediate values of $\langle k^{MF} \rangle^{blob}$ and $k_{blob} \times N_{blob}$ were obtained in Figure 2.

The trends shown in Figures 1 and 2 indicate that $\langle k^{MF} \rangle$ provides a reasonable representation of the internal dynamics of end-labeled and randomly labeled polymers when compared with the results obtained with well-established models. It is now used to probe the internal dynamics of two end-labeled types of dendrons.

MF Analysis of the Fluorescence Decays Acquired with the Pyrene End-Labeled Dendrons. The fluorescence decays acquired for the pyrene monomer and excimer of the PP- and PA-based dendrons were fitted according to the MF analysis. The results of these analyses are listed in Tables S1−3. To date, the MF analysis represents the only procedure available in the literature that can be employed to draw quantitative information about the internal dynamics of dendrons end-labeled with pyrene.[5,26] A plot of $\langle k^{MF} \rangle$ versus generation number is shown in Figure 3.
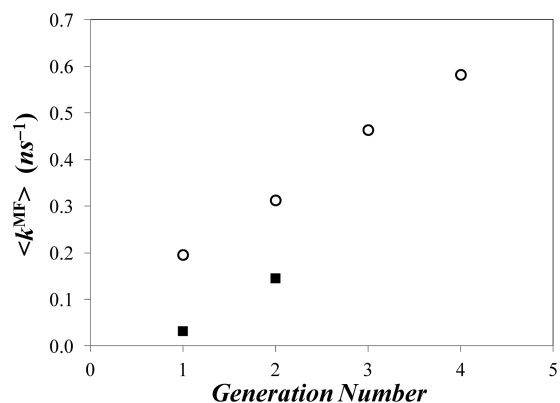

Figure 3. Plot of $\langle k^{MF} \rangle$ versus generation number for (○) PP- and (■) PA-based dendrons in tetrahydrofuran. [Py] = 2.5×10^{-6} mol·L^{-1}.

Although the trend of $\langle k^{MF} \rangle$ versus generation number for the PP-dendrons has been reported earlier,[26] it is the first time that this trend is being compared to that obtained with another type of dendron. The rigid phenyl building blocks constituting PA-G1-BuPy$_2$ and PA-G2-BuPy$_4$ hinder substantially excimer formation resulting in a much smaller $\langle k^{MF} \rangle$ value for a given generation. It was unfortunate that the crowded and rigid environment of the PA-dendrons prevented the successful labeling of the higher generation dendrons with 1-pyrenebutanol. Careful reading of papers devoted to the preparation of PA-dendrons labeled with pyrene published in the literature indicates that this problem is not uncommon.[39,40] The value of $\langle k^{MF} \rangle$ for PA-G1-BuPy$_2$ and PA-G2-BuPy$_4$ was found to be 1.7 $\times 10^8$ s^{-1} smaller than the PP-based dendrons for the same generation number. It would be interesting to investigate whether this difference in $\langle k^{MF} \rangle$ remains the same for higher

generation dendrons and whether it reflects the difference in chemical structure between the PP- and PA-based dendrons end-labeled with pyrene.

■ DISCUSSION

On the one hand, excimer formation of any pyrene-labeled macromolecule (PLM) can be characterized qualitatively from the ratio of the steady-state (SS) fluorescence of its excimer (I_E) over that of its monomer (I_M) by using the $(I_E/I_M)^{SS}$ ratio. On the other hand, the time scale over which pyrene excimer formation takes place is characterized by time-resolved fluorescence, but the quantitative analysis of the fluorescence decays requires a model. Unfortunately, models that have been developed to fit the decays of PLMs are conceptually different and can only be applied to the precise macromolecular architecture for which they were designed. As we have mentioned earlier, Birks' scheme is only applicable to monodisperse short end-labeled linear polymers,[1,7−11] whereas the FBM is used with linear chains randomly labeled with pyrene.[3,15−20] The DMD model was derived to describe excimer formation for short alkyl chains end-labeled with pyrene.[12−14,27] In contrast to these models, which apply to specific PLMs, the MF analysis can be employed to fit the decays of any PLM, and as Figures 1−3 suggest, it provides relevant information about the internal dynamics of a given PLM, which compares very well with that provided by the more specific models. In effect, the versatility of the MF analysis implies that it could be used to probe the dynamics of pyrene excimer formation in the same comprehensive manner as the $(I_E/I_M)^{SS}$ ratio obtained by steady-state fluorescence is being used to characterize the efficiency of pyrene excimer formation for any PLM. The following argument demonstrates that this is indeed the case, and that contrary to the $(I_E/I_M)^{SS}$ ratio whose experimental determination is subject to a number of complications,[43] information obtained from the MF analysis is impervious to the nature of the pyrene derivative used to label the macromolecule and yields an absolute value of the I_E/I_M ratio.

The MF analysis of the pyrene monomer and excimer decays yields the molar fractions f_{diff}, f_{free}, f_{E0}, and f_D of the pyrene species Py^*_{diff}, Py^*_{free}, E0*, and D*, respectively. In turn, these fractions can be combined with the rate constant $\langle k^{MF} \rangle$ and the lifetimes $\langle \tau \rangle$, τ_M, τ_{E0}, and τ_D to yield the $(I_E/I_M)^{SPC}$ ratio whose expression is shown in eq 4.

$$\left(\frac{I_E}{I_M}\right)^{SPC} =$$

$$\frac{f_{diff} \times \langle k^{MF} \rangle \times \tau_{E0} \times \langle \tau \rangle + f_{E0} \times \tau_{E0} + f_D \times \tau_D}{f_{diff} \times \langle \tau \rangle + f_{free} \times \tau_M} \quad (4)$$

Under the condition that all excited pyrenes form excimer by diffusion exclusively, then f_{diff} equals unity, the fractions f_{free}, f_{E0}, and f_D equal zero, and eq 4 predicts that $(I_E/I_M)^{SPC}_{f_{free}=0}$ equals the product $\langle k \rangle \times \tau_{E0}$. This result is reassuring as similar relationships have been proposed for excimer formation in solution through the diffusive encounters of molecular pyrene free in solution[28] or covalently bound onto a linear polymer.[1,6,41,42] Eq 4 was used for all constructs listed in Table 1 except for the CoAm-PS-MPy series and the PA-dendrons for which a slightly modified version of eq 4 was used (see eq S6 in SI for more details).

The fluorescence spectra and decays of the samples listed in Table 1 were analyzed to yield their $(I_E/I_M)^{SS}$ and $(I_E/I_M)^{SPC}$ ratios, which were compared in Figure 4. The $(I_E/I_M)^{SS}$ and
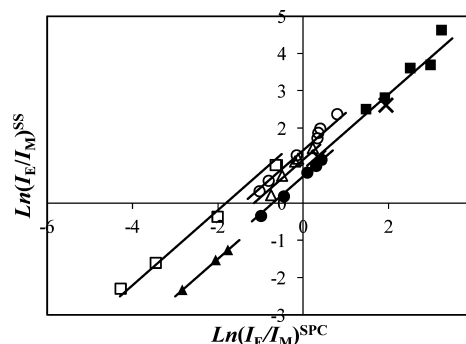
Figure 4. Comparison of the $(I_E/I_M)^{SS}$ and $(I_E/I_M)^{SPC}$ ratios obtained for the (■) PP- and (×) PA-dendrons, and the samples CoEs-PS-BuPy (●), PS-BuPy$_2$ (▲), CoEt-PS-MPy (○), and CoAm-PS-MPy (Δ) in tetrahydrofuran. [Py] = 2.5 × 10$^{−6}$ mol·L$^{−1}$. Lines with slopes equal to unity have been drawn through the data points to guide the eye.

$(I_E/I_M)^{SPC}$ ratios cluster along straight lines having a slope of unity but are shifted up and down by a set value depending on the pyrene derivative used to prepare the macromolecular construct. The discrepancy between the trends is due to differences in fluorescence intensity at 375 nm used to determine the I_M in the $(I_E/I_M)^{SS}$ ratio because the $S_{1,0} \rightarrow S_{0,0}$ transition is partially and fully allowed for the 1-pyrenemethyl bearing a heteroatom in the β-position and 1-pyrenebutyl derivatives, respectively.[11] This is illustrated in Figure S3 in the SI, where the fluorescence spectra of a CoEs-PS-BuPy and CoEt-PS-MPy sample labeled with, respectively, 3.1 and 2.7 mol % of pyrene are shown side by side. Although the samples are chemically identical, CoEt-PS-MPy seems to form much more excimer relative to the monomer than CoEs-PS-BuPy. Consequently, the $(I_E/I_M)^{SS}$ ratio is inherently larger for the PEO-MPy$_2$, CoEt-PS-MPy, and CoAm-PS-MPy samples, which were labeled with a 1-pyrenemethyl moiety, as found experimentally in Figure 4. The long butyl linker insulates pyrene more efficiently so that the trends obtained in Figure 4 with the 1-pyrenebutyl derivative are much better aligned with one another than those obtained with the 1-pyrenemethyl derivative.

The linear relationship obtained between the $(I_E/I_M)^{SS}$ and $(I_E/I_M)^{SPC}$ ratios indicates that both quantities are equivalent. Even though all fluorescence spectra were acquired in a same laboratory, thereby avoiding many of the pitfalls associated with the analysis of steady-state fluorescence spectra acquired in different laboratories,[43] little can be done to account for the inherent differences in I_M values obtained with different pyrene derivatives (see Figure S3). Interestingly, the $(I_E/I_M)^{SPC}$ ratio is not affected by the many complications that plague the determination of the $(I_E/I_M)^{SS}$ ratio, as it deals with absolute quantities (see eq 4). It takes, thus, an absolute value that can be reproduced in any other laboratory.

The efficiency of pyrene excimer formation for PLMs in solution depends on the local pyrene concentration $[Py]_{loc}$ inside the solution volume occupied by the macromolecule and the polymer flexibility.[1,3−5,40,41] In this respect, Figure 4 highlights how the molecular architecture affects the efficiency of excimer formation. Considering the trend obtained with the

1-pyrenebutyl derivative, the PS-BuPy$_2$ samples where the pyrene pendants are held apart by the chain yield the smallest I_E/I_M ratios, although their pyrene content λ_{Py} in Table 1 is similar to that of the randomly labeled polymers CoEs-PS-BuPy. For both the PS-BuPy$_2$ and CoEs-PS-BuPy series, the $(I_E/I_M)^{SS}$ and $(I_E/I_M)^{SPC}$ ratios increase with λ_{Py}, as expected, because a larger λ_{Py} value results in a larger $[Py]_{loc}$. Yet the dendrons having a similar λ_{Py} value for all generations see their $(I_E/I_M)^{SS}$ and $(I_E/I_M)^{SPC}$ ratios increase linearly with increasing generation number, a consequence of the increased branching.[26] The CoEt-PS-MPy and CoAm-PS-MPy series having a similar architecture and being both labeled with a 1-pyrenemethyl derivative yield similar $(I_E/I_M)^{SS}$ and $(I_E/I_M)^{SPC}$ values, which are offset from those obtained with the constructs labeled with a 1-pyrenebutyl linker due to the different spectral features shown in Figure S3.

Both the $(I_E/I_M)^{SS}$ and $(I_E/I_M)^{SPC}$ ratios and the average rate constant of excimer formation $\langle k^{MF} \rangle$ are measures of the efficiency of excimer formation. Consequently, the $(I_E/I_M)^{SPC}$ ratio was plotted as a function of $\langle k^{MF} \rangle$ in Figure 5. Except for
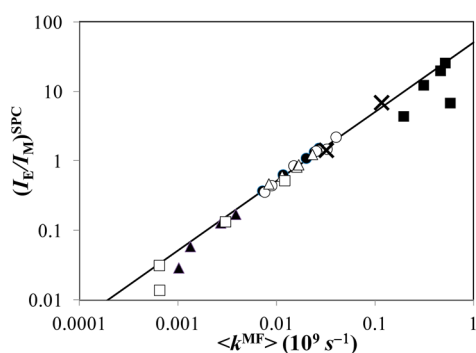

Figure 5. Comparison of the $(I_E/I_M)^{SPC}$ ratios with the $\langle k^{MF} \rangle$ values obtained for the (■) PP- and (✕) PA-dendrons, and the samples CoEs-PS-BuPy (●), PS-BuPy$_2$ (▲), CoEt-PS-MPy (○), CoAm-PS-MPy (△), and PEO-MPy$_2$ (□) in tetrahydrofuran. [Py] = 2.5×10^{-6} mol·L^{-1}.

the pyrene-labeled dendrimers and the end-labeled linear chains whose $(I_E/I_M)^{SPC}$ ratios showed substantial scatter, $(I_E/I_M)^{SPC}$ was found to increase linearly with increasing $\langle k^{MF} \rangle$ as eq 4 predicts if f_{diff} equals unity and all other molar fractions f_{free}, f_{E0}, and f_D equal 0. Indeed, f_{diff} is always larger than 0.80 in Table S3, except for the longest PS-BuPy$_2$ and PEO-MPy$_2$ samples, which indicates that the pyrene excimer is formed essentially by diffusion, as would be expected in tetrahydrofuran, which is a good solvent for pyrene. However, earlier studies have pointed out that the $(I_E/I_M)^{SPC}$ ratio obtained with pyrene-labeled dendrimers is highly sensitive to unattached pyrene labels even though f_{free} for these samples is smaller than 0.03.[5,26,32]

Also, a recent study has indicated that as the chain length of an end-labeled polymer increases, the excited pyrene located at one end of the polymer can no longer probe the entire polymer coil and emits with the natural lifetime of the monomer.[11] This phenomenon leads to an increase in f_{free}, which results in a decrease of the $(I_E/I_M)^{SPC}$ ratio, while $\langle k^{MF} \rangle$ tends to a constant value, as observed in Figure 5 for PS-BuPy$_2$ and PEO-MPy$_2$. As can be seen in Figure 6, setting f_{free} equal to 0.0 in eq 4 yields a perfect trend, where the $(I_E/I_M)^{SPC}_{f_{free}=0}$ ratio of all pyrene-labeled constructs listed in Table 1 increases linearly with increasing
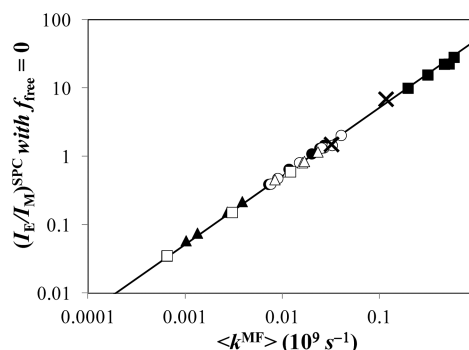

Figure 6. Comparison of the $(I_E/I_M)^{SPC}_{f_{free}=0}$ ratios with the $\langle k^{MF} \rangle$ values obtained for the (■) PP- and (✕) PA-dendrons, and the samples CoEs-PS-BuPy (●), PS-BuPy$_2$ (▲), CoEt-PS-MPy (○), CoAm-PS-MPy (△), and PEO-MPy$_2$ (□) in tetrahydrofuran. [Py] = 2.5×10^{-6} mol·L^{-1}.

$\langle k^{MF} \rangle$ with a slope τ_{E0} of 51 ns, a reasonable value for the pyrene excimer lifetime in tetrahydrofuran.[28]

It might first seem inconsistent that the $(I_E/I_M)^{SS}$ and $(I_E/I_M)^{SPC}$ ratios, which show such good correlations with one another in Figure 4, would yield a more scattered $(I_E/I_M)^{SPC}$ versus $\langle k^{MF} \rangle$ trend in Figure 5, as observed for the dendrimers and the end-labeled linear chains. Yet, this result is expected. As a matter of fact, the $(I_E/I_M)^{SS}$ and $(I_E/I_M)^{SPC}$ ratios both take into account the contributions of all pyrene species found in solution including that of Py^*_{free}, whereas $\langle k^{MF} \rangle$ is the average rate constant of excimer formation for those pyrenes that form excimer by diffusion, namely, the Py^*_{diff} species. Thus, $(I_E/I_M)^{SS}$ and $(I_E/I_M)^{SPC}$ are expected to behave differently from $\langle k^{MF} \rangle$ if pyrene species other than Py^*_{diff} can be found in solution, as is the case for the pyrene-labeled dendrimers, where the presence of minute amounts of Py^*_{free} has a dramatic effect on the $(I_E/I_M)^{SS}$ and $(I_E/I_M)^{SPC}$ ratios.[5,26,32] The trend shown in Figure 6 indicates that excimer formation is the most and the least efficient for the highly branched dendritic and the end-labeled polystyrene samples, respectively. All linear polystyrenes randomly labeled with pyrene yield similar $(I_E/I_M)^{SPC}$ ratios and $\langle k^{MF} \rangle$ values, which are intermediate between those obtained for the end-labeled polystyrenes and the highly branched dendrons.

Most importantly, Figure 6 demonstrates that the internal dynamics of any PLM can be compared to those of the macromolecules listed in Table 1, as long as the pyrene monomer and excimer fluorescence decays acquired with PLMs are analyzed globally in a manner that accounts for all pyrene species in solution quantitatively as the MF analysis does. For instance, the $(I_E/I_M)^{SPC}$ ratios determined with the MF and FBM have been shown to yield equivalent results in cases where the FBM applies (see Figure 2 and ref 30). The plot shown in Figure 6 spans more than 3 orders of magnitude in terms of the dynamic range of $(I_E/I_M)^{SPC}_{f_{free}=0}$ ratios and $\langle k^{MF} \rangle$ values. This represents the widest range of $(I_E/I_M)^{SPC}_{f_{free}=0}$ ratios and $\langle k^{MF} \rangle$ values over which the dynamics of PLMs have ever been compared. Finally, the trend shown in Figure 6 represents the only example in the literature, where the I_E/I_M ratios of different PLMs are directly compared.

Critical Appraisal of the Different Models Currently Used to Study Pyrene Excimer Formation in Pyrene-Labeled Macromolecules. The trend shown in Figure 6 conveys the impression that it represents an absolute rule

obeyed by any PLM. In turn, this impression unavoidably leads to question why such a seemingly general trend would have never been reported earlier after close to 40 years of investigations devoted to probing pyrene excimer formation in PLMs. This legitimate concern can be addressed by reviewing the various developments that contributed to the field as is being done hereafter.

Following the demonstration by Zachariasse and Kühnle (ZK) in 1976 that the process of pyrene excimer formation probed by steady-state fluorescence (SSF) provided valuable information about the conformation of a series of pyrene end-labeled alkyl chains,[12] the molecular architecture adopted in the ZK study was quickly applied in 1977 by Perico and Cuniberti to study a series of pyrene end-labeled poly(ethylene oxide)s by SSF.[6] This study reported the first example where $(I_E/I_M)^{SS}$ was found to decrease as a function of polymer chain length (N). In 1980, Winnik et al. used time-resolved fluorescence (TRF) to acquire the pyrene monomer and excimer fluorescence decays of a series of pyrene end-labeled polystyrenes.[7] Applying Birks' scheme to analyze the decays, they obtained for the first time a direct measure of the rate constant of pyrene excimer formation or end-to-end cyclization (k_{cy}) which decreased strongly with polymer chain length as $N^{-1.6}$ and showed that k_{cy} was proportional to $(I_E/I_M)^{SS}$. This study led to the rapid development of the use of TRF to obtain k_{cy} for pyrene end-labeled polymers.[1,6–11,18,40–60] Unfortunately, as the study of PLMs was extended to polymeric architectures more representative of those encountered in polymer science that differ from pyrene end-labeled monodisperse polymers, it became ever clearer that handling the kinetics of pyrene excimer formation with a single pyrene excimer formation rate constant as done in Birks' scheme was unsatisfactory.[61,62] Macromolecules bearing more than two pyrene pendants generated a distribution of rate constants corresponding to the distribution of chain lengths separating every two pyrene labels and the fluorescence decays needed to be fitted with more than the two exponentials required by Birks' scheme.[1,28] Considering the well-known uncertainties associated with the analysis of fluorescence decays with sums of exponentials,[63,64] the scientific community held the view that only qualitative information could be retrieved about the internal dynamics of a macromolecule labeled with more than two pyrenes. Although not explicitly stated, this point of view was reflected in the 1993 review by Winnik,[2] which described a large number of qualitative results obtained with a wide variety of pyrene-labeled macromolecules. Since no model could handle these complex fluorescence decays, no equation existed to fit the monomer and excimer decays acquired with these pyrene-labeled macromolecules, and both $(I_E/I_M)^{SPC}$ and $(I_E/I_M)^{SPC}_{f_{free}=0}$ could not be determined and a plot such as the one shown in Figure 6 could not be obtained.

To the best of our knowledge, the first successful attempt made at fitting sets of pyrene monomer and excimer fluorescence decays that did not obey Birks' scheme was achieved by applying the DMD model to the decays of 1,3-di(1-pyrenyl)propane where excimer formation occurred in a nonideal manner within a highly constrained geometry.[65] According to the DMD model, an excited monomer can form two excimers with two rate constants, and these two excimers can dissociate or fluoresce with two dissociation rate constants and lifetimes, respectively. These conditions lead to a set of three differential equations that can be handled by using a matrix-based formalism. The mathematical derivation leads to the conclusion that the monomer and excimer decays are a sum of three exponentials that share the same decay times but have different pre-exponential factors. Interestingly, this derivation does not yield a mathematical expression that would describe the monomer and excimer fluorescence decays as done in Birks' scheme and, thus, cannot yield an expression of $(I_E/I_M)^{SPC}$ and $(I_E/I_M)^{SPC}_{f_{free}=0}$. Within the framework of the DMD model, the decay times and pre-exponential factors retrieved from the triexponential global analysis of the fluorescence decays are linear functions of the kinetic parameters that describe the process of pyrene excimer formation. Because the exponentials are the same in the monomer and excimer fluorescence decays, three decay times and six pre-exponential factors (3 for the monomer decay and 3 for the excimer decay) are required, resulting in nine ($3 \times n = 9$, where n is the number of exponentials) floating parameters that are optimized with no constraint other than that the fit of the decay is good. The nine floating parameters retrieved from the fit are then optimized to yield the kinetic parameters. While the procedure associated with the DMD model has proved its worth for pyrene-labeled macromolecular constructs forming excimer with a finite number (=2) of excimer formation rate constants,[48,65–68] its application to polymeric systems forming pyrene excimer with a distribution of rate constants seemed more problematic.[69] This is illustrated in the following example.

The DMD model was applied to analyze the monomer and excimer fluorescence decays acquired with an aqueous solution of poly(acrylic acid) randomly labeled with pyrene (sample = PAAMePy(2)52).[69] Because the polymers had a low labeling level, the species Py^*_{free} needed to be accounted for and the monomer and excimer fluorescence decays were fitted with four coupled exponentials resulting in $3 \times 4 = 12$ floating parameters. The results of this analysis are presented in Table 2. The long decay time τ_4 was attributed to the natural lifetime

Table 2. Pre-Exponential Factors and Decay Times Retrieved from the Tetraexponential Global Analysis of the Pyrene Monomer and Excimer Decays of PAAMePy(2)52 Conducted in Ref 69

decay times (ns)	$\tau_1 = 7.0$	$\tau_2 = 53.5$	$\tau_3 = 104$	$\tau_4 = 220$
monomer	$a_{M1} = 0.066$	$a_{M2} = 0.164$	$a_{M3} = -0.080$	$a_{M4} = 0.771$
excimer	$a_{E1} = -0.149$	$a_{E2} = 0.719$	$a_{E3} = 0.281$	$a_{E4} = -0.024$

τ_M of the pyrenes that do not form excimer (Py^*_{free}). In turn, the other decays times and associated pre-exponential factors describe excimer formation. However, close analysis of Table 2 indicates a number of problems. First, the pre-exponential factors of the pyrene monomer should all be positive. This is not the case as a_{M3} equals -0.080. The authors quickly point out that its contribution is negligible, which is true when compared to a_{M4}, the contribution of Py^*_{free}. However, the ratio $|a_{M3}|/(a_{M1} + a_{M2} + |a_{M3}|)$ equals 0.26, which is far from negligible with respect to the other pre-exponential factors a_{M1} and a_{M2} that describe pyrene excimer formation. Thus, not only a_{M3} is negative instead of being positive, but it also represents a major contribution in the monomer decay with respect to pyrene excimer formation.

Another negative pre-exponential factor is a_{E4} that, again, is not physically possible, as it implies that the excimer fluorescence intensity is negative at long times. Because a_{M3}

and a_{E4} are off, the other parameters used to fit the decays are necessarily off as well, which in turn affects the determination of the kinetic parameters. Interestingly, these kinetic parameters were not determined in ref 69, probably due to the faulty set of parameters a_{Mi}, a_{Ei}, and τ_i, with $i = 1-3$, retrieved from the analysis and listed in Table 2. The problems highlighted in Table 2 are caused in part by the absence of equations describing the monomer and excimer decay that could be used to introduce additional constraints in the analysis program used to retrieve the pre-exponential factors and decay times from the fit of the fluorescence decays. By contrast, all analyses carried out by the Duhamel laboratory take full advantage of the mathematical expressions representing the monomer and excimer decays to optimize the pre-exponential factors and decay times of the sums of exponentials used to fit globally the monomer and excimer decays as a function of the kinetic parameters used to describe pyrene excimer formation. This procedure adds more constraint to the optimization package and ensures that anomalies such as those described in Table 2 are never a concern. These improvements have been described in detail in two recent reviews.[4,5]

Another procedure that has been introduced in the literature to deal with the multiexponential decays associated with macromolecules labeled with more than two pyrenes has been to lower the pyrene content of the macromolecule.[69,70] Because increasing the number of pyrene labels increases the number of chain lengths between every two pyrene pairs, thus, the number of pyrene excimer formation rate constants and, consequently, the number of exponentials that needs to be applied to fit the fluorescence decays,[15] the pyrene content can be lowered to such a level that a minimal number of exponentials need to be used. When this is the case, two coupled exponentials with a third exponential for Py^*_{free} fit the monomer and excimer decays well, and the pre-exponential factors and decay times retrieved from the two coupled exponentials can be interpreted according to Birks' scheme. Unfortunately, the results retrieved from this analysis conducted in a few examples[69,70] consistently yield large pyrene excimer dissociation rate constant k_{-1} that are 2−6 times larger than $5 \times 10^6 \text{ s}^{-1}$, which is the upper value typically obtained for short monodisperse polymers end-labeled with pyrene. Longer chains yield larger k_{-1} values due to a breakdown of Birks' scheme under these conditions, as demonstrated in a recent study.[11]

To summarize the procedures described up to this point, none of the analyses presented earlier aimed to address the inherent distribution of rate constants resulting from the distribution of chain lengths separating the pyrene pendants covalently attached to a macromolecule. This is unfortunate for the vast majority of pyrene-labeled macromolecules contain more than two pyrene labels which are not separated by a set chain length. Furthermore, these analyses have been found to yield kinetic parameters which are inconsistent with commonly accepted facts about the process of pyrene excimer formation, most importantly that k_{-1} takes values smaller than $5 \times 10^6 \text{ s}^{-1}$.

In contrast with these earlier studies, the FBM was the first model specifically designed to handle the distribution of rate constants encountered in polymers randomly labeled with pyrene. After demonstrating in 1999 that the FBM could satisfyingly handle the monomer decays acquired with a series of polystyrenes randomly labeled with pyrene,[15] the analysis program was improved to enable the global analysis of the monomer and excimer fluorescence decays.[71] Because the FBM provided explicit expressions for the time-dependent behavior

of the pyrene monomer and excimer given in eqns S11 and S12, an expression of $(I_E/I_M)^{SPC}$ and $(I_E/I_M)^{SPC}_{f_{free}=0}$ could be derived for polymers randomly labeled with pyrene.[72] However, the FBM could not handle all pyrene-labeled macromolecules as the labeling of macromolecules is not always conducted in a random manner, a prerequisite for application of the FBM. After noting that any fluorescence decay could be fitted with a sum of exponentials, the MF analysis was introduced where the pyrene monomer is fitted with a sum of exponentials and an expression for the excimer decay is obtained using the same procedure applied for the FBM.[31] Here again, mathematical expressions could be derived for the pyrene monomer and excimer decay, as shown in eqns S1 and S2, which could be integrated to yield $(I_E/I_M)^{SPC}$ and $(I_E/I_M)^{SPC}_{f_{free}=0}$, as described in eq 4.[26,32,33] The main limitation of the MF analysis is that it yields an average $\langle k \rangle$ value, which loses some of the molecular details of pyrene excimer formation that would be provided otherwise by an analysis based on Birks' scheme, the DMD model, or the FBM. However, this limitation is compensated by the demonstrated applicability of the MF analysis to describe the internal dynamics of a presently unmatched variety of pyrene-labeled macromolecular constructs,[26,31,33−35,73] as further illustrated in this report. The MF analysis achieves this result by capturing the main features of the decays and summarizing them into a small set of parameters which are the average rate constant of pyrene excimer formation $\langle k \rangle$, the excimer lifetime τ_{E0}, and the molar fractions of the different species that fluoresce in solution.

Whereas the studies conducted with PLMs using models other than the FBM or MF have been applied to a limited number of PLMs and yield sets of kinetic parameters that are questionable and somewhat inconsistent with what is generally accepted about pyrene excimer formation, the FBM and MF analyses have been applied successfully to a wide variety of pyrene-labeled macromolecular constructs as demonstrated by this report and yield sets of kinetic parameters consistent with the established consensus about pyrene excimer formation and expectations about the PLM investigated. Furthermore, FBM and MF analyses are currently the only procedures that provide mathematical expressions for the pyrene monomer and excimer that can be applied directly to fit the complex fluorescence decays acquired with a wide range of PLMs and to derive the only expressions of $(I_E/I_M)^{SPC}$ and $(I_E/I_M)^{SPC}_{f_{free}=0}$ available in the literature for PLMs that contain more than two pyrenes attached at two specific positions of a macromolecule.

■ CONCLUSIONS

This study demonstrates that the MF analysis of the fluorescence decays of PLMs appears to be a powerful and versatile procedure to gain information about the internal dynamics of any type of PLM. Comparison of k_{cy} and $\langle k^{MF} \rangle$ obtained from, respectively, the Birks' scheme and MF analysis, yielded trends for the end-labeled polymers that were similar and, at the very least, provided identical information about the macromolecules studied, namely, that $\langle k^{MF} \rangle$ decreases as a power law with increasing chain length and that $\langle k^{MF} \rangle$ for relatively stiff polystyrene is much smaller than for comparatively flexible PEO. It was also shown that $\langle k^{MF} \rangle^{blob}$ derived from $\langle k^{MF} \rangle$ yielded identical trends for the randomly labeled polystyrenes with respect to the $k_{blob} \times N_{blob}$ values retrieved from the more traditional FBM analysis. In particular, $\langle k^{MF} \rangle^{blob}$ reflected satisfyingly the nature of the spacer connecting the

pyrene derivative to the polymer backbone. Finally, the MF analysis was shown to probe the end-group dynamics of pyrene end-labeled dendrons in a manner that reflected the molecular flexibility expected from the chemical composition of the dendrons.

The overall agreement between the trends obtained with the MF analysis on the one hand and the more traditional models on the other hand is quite remarkable considering that the MF analysis is conceptually different from the other models, in particular, by making no assumption about the mathematical details used to model pyrene excimer formation. The MF analysis also accounts quantitatively for all pyrene species present in solution, most importantly the Py^*_{free} species. This represents an advantage over other analytical procedures in cases where elimination of all unattached dyes from PLMs is challenging and the fluorescence signal is sensitive to their contribution, as was found with the pyrene-labeled dendrons. The MF analysis takes also advantage of the design of our analysis programs where the monomer and excimer fluorescence decays are fitted globally and the decay times and pre-exponential factors in the sum of exponentials are optimized as a function of the kinetic parameters involved in the kinetic schemes representing pyrene excimer formation. This ensures that erroneous results without physical meaning such as those reported in Table 2 are avoided. Last, but not least, the quantities $(I_E/I_M)^{SPC}_{f_{free}=0}$ and $\langle k^{MF} \rangle$ determined by the MF analysis are absolute and can be reproduced in any laboratory.

The versatility and generality of the MF analysis were further illustrated by demonstrating that a plot of $(I_E/I_M)^{SPC}_{f_{free}=0}$ versus $\langle k^{MF} \rangle$ generates a master curve in Figure 6 along which all PLMs studied converge without a single exception. Thus, the master curve in Figure 6 constitutes a calibration curve against which the internal dynamics of any other PLM can now be gauged. It should prove highly valuable to the many scientists who use pyrene excimer formation to probe the internal dynamics of macromolecules.

Finally, it must be pointed out that although this report has demonstrated the general applicability of the MF analysis to study the internal dynamics of PLMs, its realm of application is actually much broader. The MF analysis also yields the fractions weighed by the molar absorption coefficient and radiative rate constant of the different pyrene species contributing to the monomer and excimer fluorescence decays.[31] In turn, these fractions can be used to determine the actual molar fractions of the pyrene species. This feature allowed some of us to assess the extreme sensitivity of the $(I_E/I_M)^{SS}$ and $(I_E/I_M)^{SPC}$ ratios obtained for pyrene end-labeled dendrimers to the presence of free pyrene labels.[26] It led to the determination of the molar absorbance coefficient of pyrene aggregates generated by a poly(ethylene oxide) labeled at one end with pyrene.[73] It was applied to determine the concentration of unmicellized surfactant for a pyrene-labeled gemini surfactant which demonstrated that above the CMC of the surfactant, the concentration of unassociated surfactant remains constant and equals the CMC.[33] More recent experiments have shown that the MF analysis can be employed not only to study pyrene excimer formation, but for any fluorescence experiment dealing with two communicating fluorescence channels, such as in a FRET experiment. In particular, the MF analysis was successfully applied to probe the kinetics of FRET between an excited pyrene donor to a ground-state porphyrin acceptor in two pyrene dendronized porphyrin constructs.[31] These

earlier results together with those presented in this report further demonstrate that the MF analysis is a powerful and versatile analytical procedure to investigate the behavior of PLMs in solution.

■ ASSOCIATED CONTENT

ⓢ Supporting Information

Fluorescence spectra of two polystyrene samples randomly labeled with a 1-pyrenemethyl and 1-pyrenebutyl derivative; Detailed description of the models used to fit the fluorescence decays; Tables of the pre-exponential factors and decay times retrieved from the analyses. This material is available free of charge via the Internet at http://pubs.acs.org.

■ AUTHOR INFORMATION

Notes
The authors declare no competing financial interest.

■ ACKNOWLEDGMENTS

■ REFERENCES

(1) Winnik, M. A. *Acc. Chem. Res.* **1985**, *18*, 73−79.
(2) Winnik, F. M. *Chem. Rev.* **1993**, *93*, 587−614.
(3) Duhamel, J. *Acc. Chem. Res.* **2006**, *39*, 953−960.
(4) Duhamel, J. *Langmuir* **2012**, *28*, 6527−6538.
(5) Duhamel, J. *Polymers* **2012**, *4*, 211−239.
(6) Cuniberti, C.; Perico, A. *Eur. Polym. J.* **1977**, *13*, 369−374.
(7) Winnik, M. A.; Redpath, T.; Richards, D. H. *Macromolecules* **1980**, *13*, 328−335.
(8) Svirskaya, P.; Danhelka, J.; Redpath, A. E. C.; Winnik, M. A. *Polymer* **1983**, *24*, 319−322.
(9) Ghiggino, K. P.; Snare, M. J.; Thistlethwaite, P. J. *Eur. Polym. J.* **1985**, *21*, 265−272.
(10) Boileau, S.; Méchin, F.; Martinho, J. M. G.; Winnik, M. A. *Macromolecules* **1989**, *22*, 215−220.
(11) Chen, S.; Duhamel, J.; Winnik, M. A. *J. Phys. Chem. B* **2011**, *115*, 3289−3302.
(12) Zachariasse, K.; Kühnle, W. *Z. Phys. Chem.* **1976**, *101*, 267−276.
(13) Kanaya, T.; Goshiki, K.; Yamamoto, M.; Nishijima, Y. *J. Am. Chem. Soc.* **1982**, *104*, 3580−3587.
(14) Zachariasse, K. A.; Maçanita, A. L.; Kühnle, W. *J. Phys. Chem. B* **1990**, *103*, 9356−9365.
(15) Mathew, A.; Siu, H.; Duhamel, J. *Macromolecules* **1999**, *32*, 7100−7108.
(16) Kanagalingam, S.; Spartalis, J.; Cao, T.-C.; Duhamel, J. *Macromolecules* **2002**, *35*, 8571−8577.
(17) Picarra, S.; Relogio, P.; Afonso, C. A. M.; Martinho, J. M. G.; Farinha, J. P. S. *Macromolecules* **2003**, *36*, 8119−8129.
(18) Ingratta, M.; Hollinger, J.; Duhamel, J. *J. Am. Chem. Soc.* **2008**, *130*, 9420−9428.
(19) Teertstra, S. J.; Lin, W. Y.; Gauthier, M.; Ingratta, M.; Duhamel, J. *Polymer* **2009**, *50*, 5456−5466.
(20) Yip, J.; Duhamel, J.; Qiu, X. P.; Winnik, F. M. *Macromolecules* **2011**, *44*, 5363−5372.
(21) Wilken, R.; Adams, J. *Macromol. Rapid Commun.* **1997**, *18*, 659−665.
(22) Baker, L. A.; Crooks, R. M. *Macromolecules* **2000**, *33*, 9034−9039.
(23) Brauge, L.; Caminade, A.-M.; Majoral, J.-P.; Slomkowski, S.; Wolszczak, M. *Macromolecules* **2001**, *34*, 5599−5606.
(24) Wang, B.-B.; Zhang, X.; Jia, X.-R.; Li, Z.-C.; Ji, Y.; Yang, L.; Wei, Y. *J. Am. Chem. Soc.* **2004**, *126*, 15180−15194.
(25) Cicchi, S.; Fabbrizzi, P.; Ghini, G.; Brandi, A.; Foggi, P.; Marcelli, A.; Righini, R.; Botta, C. *Chem.—Eur. J.* **2009**, *15*, 754−564.

(26) Yip, J.; Duhamel, J.; Bahun, G. J.; Adronov, A. *J. Phys. Chem. B* **2010**, *114*, 10254−10265.

(27) Zachariasse, K. A.; Busse, R.; Duveneck, G.; Kühnle, W. *J. Photochem.* **1985**, *28*, 237−253.

(28) Birks, J. B. *Photophysics of Aromatic Molecules*; Wiley: New York, 1970; p 301.

(29) Ingratta, M.; Duhamel, J. *Macromolecules* **2007**, *40*, 6647−6657.

(30) Bahun, G. J.; Adronov, A. *J. Polym. Sci., Part A: Polym. Chem.* **2010**, *48*, 1016−1028.

(31) Zaragoza-Galán, G.; Fowler, M.; Duhamel, J.; Rein, R.; Solladié, N.; Rivera, E. *Langmuir* **2012**, *28*, 11195−11205.

(32) Ingratta, M.; Mathew, M.; Duhamel, J. *Can. J. Chem.* **2010**, *88*, 217−227.

(33) Siu, H.; Duhamel, J. *J. Phys. Chem. B* **2005**, *109*, 1770−1780.

(34) Chen, S.; Duhamel, J.; Bahun, G.; Adronov, A. *J. Phys. Chem. B* **2011**, *115*, 9921−9929.

(35) Keyes-Baig, C.; Duhamel, J.; Wettig, S. *Langmuir* **2011**, *27*, 3361−3371.

(36) Press, W. H.; Flannery, B. P.; Teukolsky, S. A.; Vetterling, W. T. *Numerical Recipes. The Art of Scientific Computing (Fortran Version)*; Cambridge University Press: Cambridge, 1992.

(37) Svirskaya, P.; Danhelka, J.; Redpath, A. E. C.; Winnik, M. A. *Polymer* **1983**, *24*, 319−322.

(38) Ingratta, M.; Duhamel, J. *J. Phys. Chem. B* **2009**, *113*, 2284−2292.

(39) Stewart, G. M.; Fox, M. A. *J. Am. Chem. Soc.* **1996**, *118*, 4354−4360.

(40) Vanjinathan, M.; Lin, H.-C.; Nasar, A. S. *Macromol. Chem. Phys.* **2011**, *212*, 849−859.

(41) Cuniberti, C.; Perico, A. *Eur. Polym. J.* **1980**, *16*, 887−893.

(42) Cuniberti, C.; Perico, A. *Prog. Polym. Sci.* **1984**, *10*, 271−316.

(43) Steady-state fluorescence spectra depend on the slit width used for the excitation and emission monochromators, the geometry (front-face or right angle) used for the acquisition, and the sensitivity of the photomultiplier tube with wavelength and the procedure used to determine the $(I_E/I_M)^{SS}$ ratios.

(44) Cheung, S.-T.; Winnik, M. A.; Redpath, A. E. C. *Macromol. Chem. Phys.* **1982**, *183*, 1815−1824.

(45) Redpath, A. E. C.; Winnik, M. A. *J. Am. Chem. Soc.* **1982**, *104*, 5604−5607.

(46) Winnik, M. A.; Redpath, A. E. C.; Paton, K.; Danhelka, J. *Polymer* **1984**, *25*, 91−99.

(47) Boileau, S.; Méchin, F.; Martinho, J. M. G.; Winnik, M. A. *Macromolecules* **1989**, *22*, 215−220.

(48) Slomkowski, S.; Winnik, M. A. *Macromolecules* **1986**, *19*, 500−501.

(49) Xu, H.; Martinho, J. M. G.; Winnik, M. A.; Beinert, G. *Makromol. Chem.* **1989**, *190*, 1333−1343.

(50) Farinha, J. P. S.; Martinho, J. M. G.; Xu, H.; Winnik, M. A.; Quirk, R. P. *J. Polym. Sci., Part B: Polym. Phys.* **1994**, *32*, 1635−1642.

(51) Martinho, J. M. G.; Reis e Sousa, A. T.; Winnik, M. A. *Macromolecules* **1993**, *26*, 4484−4488.

(52) Duhamel, J.; Khayakin, Y.; Hu, Y. Z.; Winnik, M. A.; Boileau, S.; Méchin, F. *Eur. Polym. J.* **1994**, *30*, 129−134.

(53) Lee, S.; Winnik, M. A. *Macromolecules* **1997**, *30*, 2633−2641.

(54) Lee, S.; Duhamel, J. *Macromolecules* **1998**, *31*, 9193−9200.

(55) Reis e Sousa, A. T.; Castanheira, E. M. S.; Fedorov, A.; Martinho, J. M. G. *J. Phys. Chem. A* **1998**, *102*, 6406−6411.

(56) Piçarra, S.; Gomes, P. T.; Martinho, J. M. G. *Macromolecules* **2000**, *33*, 3947−3950.

(57) Farinha, J. P. S.; Piçarra, S.; Miesel, K.; Martinho, J. M. G. *J. Phys. Chem. B* **2001**, *105*, 10536−10545.

(58) Kim, S. D.; Torkelson, J. M. *Macromolecules* **2002**, *35*, 5943−5952.

(59) Gardinier, W. E.; Bright, F. V. *J. Phys. Chem. B* **2005**, *109*, 14824−14829.

(60) Costa, T.; Seixas de Melo, J.; Burrows, H. D. *J. Phys. Chem. B* **2009**, *113*, 618−626.

(61) Winnik, M. A.; Li, X.-B.; Guillet, J. E. *Macromolecules* **1984**, *17*, 699−702.

(62) Winnik, M. A.; Egan, L. S.; Tencer, M.; Croucher, M. D. *Polymer* **1987**, *28*, 1553−1560.

(63) Lakowicz, J. R. *Principles of Fluorescence Spectroscopy*; Plenum Press: New York, 1983.

(64) James, D. R.; Ware, W. R. *Chem. Phys. Lett.* **1985**, *120*, 455−459.

(65) Zachariasse, K. A.; Busse, R.; Duveneck, G.; Kühnle, W. *J. Photochem.* **1985**, *28*, 237−253.

(66) Zachariasse, K. A.; Busse, R.; Duveneck, G.; Kühnle, W. *J. Photochem.* **1985**, *28*, 237−253.

(67) Zachariasse, K. A.; Duveneck, G. *J. Am. Chem. Soc.* **1987**, *109*, 3790−3792.

(68) Zachariasse, K. A.; Kühnle, W.; Leinhos, U.; Reynders, P.; Strikers, G. *J. Phys. Chem.* **1991**, *95*, 5476−5488.

(69) Seixas, de Melo, J.; Costa, T.; Francisco, A.; Maçanita, A. L.; Gago, S.; Gonçalves, I. S. *Phys. Chem. Chem. Phys.* **2007**, *9*, 1370−1385.

(70) Seixas de Melo, J.; Costa, T.; Miguel, M. d. G.; Lindman, B.; Schillén, K. *J. Phys. Chem.* **2003**, *107*, 12605−12621.

(71) Siu, H.; Duhamel, J. *Macromolecules* **2004**, *37*, 9287−9289.

(72) Siu, H.; Duhamel, J. *Macromolecules* **2005**, *38*, 7184−7186.

(73) Siu, H.; Duhamel, J. *J. Phys. Chem. B* **2012**, *116*, 1226−1233.